

Associations between redox-sensitive trace metals and microbial communities in a Proterozoic ocean analogue

Kathryn I. Rico^{1,2}  | Nathan D. Sheldon¹  | Lauren E. Kinsman-Costello³

¹Department of Earth and Environmental Sciences, University of Michigan, Ann Arbor, MI, USA

²Department of Earth and Planetary Sciences, McGill University, Montreal, QC, Canada

³Department of Biological Sciences, Kent State University, Kent, OH, USA

Correspondence

Nathan D. Sheldon, Department of Earth and Environmental Sciences, University of Michigan, 1100 N. University Ave Rm 2534, Ann Arbor, MI 48103, USA.
Email: nsheldon@umich.edu

Funding information

National Science Foundation; Sokol Foundation; University of Michigan

Abstract

Constraints on Precambrian ocean chemistry are dependent upon sediment geochemistry. However, diagenesis and metamorphism can destroy primary biosignatures, making it difficult to consider biology when interpreting geochemical data. Modern analogues for ancient ecosystems can be useful tools for identifying how sediment geochemistry records an active biosphere. The Middle Island Sinkhole (MIS) in Lake Huron is an analogue for shallow Proterozoic waters due to its low oxygen water chemistry and microbial communities that exhibit diverse metabolic functions at the sediment–water interface. This study uses sediment trace metal contents and microbial abundances in MIS sediments and an oxygenated Lake Huron control site (LH) to infer mechanisms for trace metal burial. The adsorption of trace metals to Mn-oxyhydroxides is a critical burial pathway for metals in oxic LH sediments, but not for the MIS mat and sediments, consistent with conventional understanding of Mn cycling. Micronutrient trace metals (e.g., Zn) are associated with organic matter regardless of oxygen and sulfide availability. Although U and V are conventionally considered to be organically complexed in suboxic and anoxic conditions, U and organic covary in oxic LH sediments, and Mn-oxyhydroxide cycling dominates V deposition in the anoxic MIS sediments. Significant correlations between Mo and organic matter across all redox regimes have major implications for our interpretations of Mo isotope systematics in the geologic record. Finally, while microbial groups vary between the sampling locales (e.g., the cyanobacteria in the MIS microbial mat are not present in LH sediments), LH and MIS ultimately have similar relationships between microbial assemblages and metal burial, making it difficult to link trace metal burial to microbial metabolisms. Together, these results indicate that bulk sediment trace metal composition does not capture microbiological processes; more robust trace metal geochemistry such as isotopes and speciation may be critical for understanding the intersections between microbiology and sediment geochemistry.

KEYWORDS

microbial mat, Proterozoic analogue, redox, trace metals

1 | INTRODUCTION

Partial oxygenation of the atmosphere ~2.34 Ga ago (the Great Oxidation Event; GOE) is widely accepted due to the disappearance

of non-mass-dependent $\Delta^{33}\text{S}$ anomalies (Farquhar, Bao, & Thiemens, 2000) as well as a variety of other observations from the sedimentary record such as the appearance of oxidized soils on land and the loss of detrital pyrite from ancient stream beds (see Lyons, Reinhard, &

Planavsky, 2014, for review). The GOE also partially oxygenated the upper parts of the Proterozoic oceans, allowing for the diversification of microbial life and evolution of eukaryotes (Knoll, 2015; Lyons et al., 2014; Planavsky et al., 2018). Our current understanding of Proterozoic ocean chemistry is largely dependent on the geochemistry of ancient sediments (e.g., Planavsky et al., 2018; Reinhard et al., 2013; Sperling, Halverson, Knoll, Macdonald, & Johnston, 2013). For example, trace metal (e.g., Mo, U) sediment geochemistry is considered a robust tool for constraining the redox chemistry of ancient oceans (e.g., Algeo & Lyons, 2006; Algeo & Maynard, 2004; Planavsky et al., 2018; Tessin, Chappaz, Hendy, & Sheldon, 2018). However, those ancient sediments may or may not include direct evidence of an active biosphere (such as stromatolites or biomarkers; e.g., Brocks et al., 2017; Noffke & Awramik, 2013) even though one is widely assumed, making it difficult to consider the role of biology when interpreting geochemical data. Therefore, modern analogues for ancient ecosystems have been used to develop hypotheses about biogeochemical cycling in the fossil record (e.g., Hamilton et al., 2017; Hasiotis, Brake, Dannelly, & Duncan, 2001; Konhauser, Phoenix, Bottrell, Adams, & Head, 2001; Rothschild, 1991). In addition, modern analogue systems are excellent models for testing the applicability of paleoproductivity and paleoredox proxies and for interpreting results in a geologic context.

This work aims to use an analogue for the Proterozoic to examine the burial pathways for trace metals across modern oxic and anoxic sediments and to consider how trace metal geochemistry is influenced by the presence of a cyanobacterial microbial mat system. The Middle Island Sinkhole (MIS), located 23 m below the surface of Lake Huron, has biotic and abiotic characteristics that make it an appropriate analogue for shallow Proterozoic ocean sites (Table 1). Low-oxygen groundwater seeps into MIS, creating an environment with lower oxygen, elevated sulfate concentration, and higher conductivity (i.e., salinity) relative to the rest of Lake Huron (Table 1). Quantitatively, the dissolved oxygen, iron, and sulfate values are similar to those reconstructed for shallow Proterozoic ocean waters (Rico & Sheldon, 2019). The groundwater layers persists <3 m above the sediment–water interface, with mixing between MIS and surrounding Lake Huron waters limited to brief periods in the summer (Biddanda et al., 2012; Ruberg et al., 2008). This water chemistry allows for the proliferation of microbial communities of diverse metabolic functions at the sediment–water interface and generally

excludes multicellular life. These microbial mats include cyanobacteria that conduct both anoxygenic and oxygenic photosynthesis, sulfur oxidizers, and reducers and Archaea (Biddanda et al., 2012; Kinsman-Costello et al., 2017; Voorhies et al., 2012).

In comparison, a fully oxygenated Lake Huron control site (LH) of comparable depth does not have a microbial mat at the sediment–water interface; instead, LH sediments have a different microbial community structure than MIS (e.g., a lack of cyanobacteria that dominate MIS microbial mats; Kinsman-Costello et al., 2017). Sediment geochemistry of these localities also varies, in that MIS sediments are enriched in macronutrients such as C, N, and P, as well as metals such as Fe, Mn, and Mo, relative to LH sediments (Kinsman-Costello et al., 2017; Nold et al., 2013; Rico & Sheldon, 2019; Rico, Sheldon, Gallagher, & Chappaz, 2019). Differences in chemistry extend to the pore waters, with inorganic nutrient concentrations of MIS pore waters higher than that of LH pore waters, and evidence for variable oxygen penetration and sulfide accumulation in MIS pore waters (Kinsman-Costello et al., 2017).

With stark differences in water chemistry, microbial community composition, and sediment geochemistry, MIS and LH serve as low-oxygen and fully oxygenated endmembers for considering how trace metals respond to different abiotic (i.e., redox chemistry) and biotic controls (i.e., microbial community composition and metabolisms). Relationships between organic matter and different types of metals—organically complexed, micronutrient, oxide-forming, and sulfide-complexed—in oxic LH and anoxic MIS serve as a test to gauge whether or not these metals are responding as expected based on their use as paleoredox and paleoproductivity proxies. Additionally, considering MIS as an analogue for Proterozoic oceans (Biddanda et al., 2012; Rico & Sheldon, 2019; Voorhies et al., 2012), MIS microbial mats can be used to determine whether trace metal geochemistry could have been influenced by microbial activity in the fossil record.

2 | METHODS

2.1 | Sample collection and processing

National Oceanic Administration Thunder Bay National Marine Sanctuary (NOAA TBNMS) scuba divers collected surficial sediment

TABLE 1 Summary of select water column and sediment parameters, comparing the Middle Island Sinkhole (MIS) to the Lake Huron control site (LH)

		MIS	LH
Water column parameters	Dissolved oxygen concentration (μM) ^{a,b}	<125	344
	Salinity (PSU) ^{a,b}	1.23	0.13
	Dissolved sulfate concentration (mM) ^{a,b}	7.8	0.15
	Dissolved iron concentration (μM) ^b	1–2	<0.1
	pH	7.3	8.3
Sediment parameters	Organic C (%) ^b	7	1.5
	Total Fe (%) ^b	1.5	1.0

^aFrom Ruberg et al. (2008) and Biddanda et al. (2012).

^bFrom Rico and Sheldon (2019).

cores from MIS ($n = 9$; $45^{\circ}11.911'N$, $83^{\circ}19.662'W$) and LH ($n = 8$; $45^{\circ}12.267'N$, $83^{\circ}19.831'W$) during September 2014 and May 2015. Sediments were collected in 20×7 cm (length \times inner diameter) clear polycarbonate tubes. In May 2015, one "long core" (30×7 cm) was also collected at MIS. Cores were immediately frozen and transported upright to the University of Michigan in Ann Arbor, MI, where they were stored at $-20^{\circ}C$. Frozen cores were sectioned via a solvent-cleaned table saw according to depth (three 1-cm sections at the top, then 3-cm intervals downcore), freeze-dried, and homogenized.

2.2 | Elemental analysis

MIS ($n = 56$) and LH ($n = 22$) samples were analyzed for metal (Mn, U, V, Cd, Zn, Ni, Cu, Fe, Mo, Al) and macronutrient (S, P) contents at ALS Laboratories in Vancouver, British Columbia (Mo and U contents previously reported in Rico et al., 2019; Fe, S, and P contents were previously reported in Rico & Sheldon, 2019). Samples (0.25 g each) were digested with perchloric, hydrofluoric, nitric, and hydrochloric acids, and concentrations were determined by inductively coupled plasma (ICP)-atomic emission spectroscopy and ICP-mass spectroscopy. OREA-45d, MRGeo08, OGeo08, and CDN-CM-34 internal standards were used to verify elemental concentrations. Relative error for major elements was $<2\%$, while relative error for trace elements was $<3\%$. Additional macronutrient contents (C_{org} and N) used in this work were determined via Elemental Analyzer, as described Rico and Sheldon (2019).

2.3 | Trace element organization

Trace metals are presented as normalized to Al content in order to represent authigenic enrichments of target elements (Van der Weijden, 2002). Al was chosen because Al contents across MIS and LH had lower variability than other immobile elements (i.e., Ti and Zr; Van der Weijden, 2002). Al-normalization was used instead of calculating detrital vs. authigenic inputs due to a lack of data on detrital inputs to the Great Lakes region. The metals selected (Mn, U, V, Cd, Zn, Ni, Cu, Mo) were divided into four categories based upon their uses as redox and productivity proxies: oxide-forming metals (e.g., Mn; Calvert & Pederson, 1993; Tribovillard, Algeo, Lyons, & Riboulleau, 2006); metals that accumulate under suboxic to anoxic conditions (U and V; Algeo & Maynard, 2004; Klinkhammer & Palmer, 1991; Tribovillard et al., 2006); metals that act as micronutrients, especially as incorporated by microbial metabolisms (Zn, Cd, Ni, and Cu; Jelen, Giovannelli, & Falkowski, 2016; Lepp, 1992; Moore, Jelen, Giovannelli, Raanan, & Falkowski, 2017; Tribovillard et al., 2006), and metals that are proxies for free sulfide availability (e.g., Mo; Erickson & Helz, 2000; Zheng, Anderson, Van Geen, & Kuwabara, 2000). It is important to note that some of these metals could belong to multiple categories (e.g., Mn is also involved photosystem II during oxygenic photosynthesis and therefore serves

as a micronutrient; Ferreira, Iverson, Maghlaoui, Barber, & Iwata, 2004), however categories are used in this work to group metals that are used similarly as paleoproxies throughout the literature (e.g., Algeo & Maynard, 2004; Tribovillard et al., 2006; Sperling et al., 2013; Miller et al., 2017; Nguyen et al., 2019). Although Fe geochemistry is also considered to be one of the most robust tools for understanding the redox chemistry of aquatic environments (Raiswell & Canfield, 2012; Raiswell et al., 2018), Fe could be placed the various categories of metals explored in this study (e.g., Fe forms oxides, is reactive to sulfide, and can be used as enzymatic cofactor across a variety of microbial metabolisms; Huerta-Diaz & Morse, 1992; Moore et al., 2017; Tessier, Fortin, Belzile, DeVitre, & Leppard, 1996). In addition, the Fe geochemistry of MIS and LH has already been explored in Rico and Sheldon (2019). Hence, discussion of Fe in this study is limited.

2.4 | Microbial community composition

Relative abundances and composition of microbial communities for MIS sediments ($n = 87$), MIS mat ($n = 17$, wherein mat is defined as 0–1 cm depth), and LH sediments ($n = 11$) were previously published by Kinsman-Costello et al. (2017); see methods therein for complete information on DNA extraction, quantification, amplification, sequencing, and taxonomic clustering.

2.5 | Ordination methods

Principal component analysis (PCA) was performed using Past 3.14 (Hammer, Harper, & Ryan, 2001) in order to (a) represent how different trace metals and macronutrients are associated with MIS mat and sediment, and LH sediment, and (b) how trace metal and macronutrient geochemistry are related to the relative abundances of major biological groups. Redundancy analysis (RDA) was also used to consider the ways in MIS and Lake Huron microbial assemblages constrain the variability in sediment geochemistry (Figure S2). RDA was carried out with the Vegan package in RStudio software version 1.1.463 (Oksanen et al., 2013). In order to demonstrate true variance in the data and account for different unit scales, all variables were standardized by z-score (see Supporting Information for details).

3 | RESULTS AND DISCUSSION

3.1 | Broad controls on trace metal burial

Independent of water column oxygen and iron measurements, the iron geochemistry of MIS and LH sediments has corroborated known water chemistries of the two locales—with MIS as lower in oxygen and rich in Fe relative to the oxic Lake Huron—providing a redox-based mechanism for the enhanced burial of macronutrients and the different species of Fe in MIS sediments relative to

LH sediments (Table 1; Rico & Sheldon, 2019). Based upon these Fe speciation results, MIS Fe geochemistry is not recording the bulk of the water column (i.e., 20 m of oxic Lake Huron water), but rather rapid transformations across the redoxcline, or the influence of early diagenesis (Rico & Sheldon, 2019). These controls on iron geochemistry could also be impacting the burial of trace metals in MIS mat and sediments.

Trace metal contents do not vary between the MIS mat and MIS sediments, but are generally higher than those of the LH sediments, with Mn as the only exception (Table 2). In MIS sediments, downcore trace metal contents do not change with depth for U, V, Ni, Cu, and Fe (Figures 1 and S1), increase in Cd and Zn with depth (Figures 1 and S1), and decrease with depth for Mo (Figure 1). Trace metal contents of LH sediments show a pattern of decreasing abundance with depth after 10 cm; however, Mn also decreases with depth in the first 3 cm (Figure 1). Principal component and correlative analyses help to determine how variable redox chemistry between LH and MIS has an impact on trace metal burial.

The PCA is used to group trace metals, macronutrients, and relative abundances of major biological groups based on their covariance across LH and MIS sediments as a function of depth. The first two components account for ~87% of the total variance: PC1 accounts for 58.2% of the variability, while PC2 accounts for 28.4%. MIS sediments and LH sediments are distributed separately across PC1, with PC1 separating LH sediments by their depth bins and PC2 separating MIS sediments by depth (Figure 2). With the exception of Mn, trace metals and macronutrients are associated with the MIS mat and sediments, rather than LH sediments (Figure 2). PC2 separates

the macronutrients and the trace metals across the MIS sediments, with trace metals associated with deeper MIS sediments, and macronutrients covarying with shallower MIS sediments and the MIS mat (0–1 cm; Figure 2). PC1 therefore effectively serves as a gradient from oxic (LH) to low-oxygen (MIS) settings, while the variance described by PC2 is dependent on the influence of the microbial mat (and associated macronutrients) in surficial MIS sediments.

In addition to PCA, RDA was considered to determine which major microbiological groups explain most of the variance in sediment geochemistry (Figure S2). RDA results indicate that the relative abundance of six microbial groups constrains 19% of the variability in sediment geochemistry. The orientation of MIS and LH depth bins, microbial groups, macronutrients, and trace metals is similar between the RDA and the PCA (Figures 2 and S2); RDA did not yield additional insight about the relationships between trace metal burial and microbial community assemblage in MIS and LH. Instead, the relationships between trace metal burial and organic matter in LH sediments, MIS sediments, and MIS sediments dominated by the microbial mat (0–3 cm depth according to $^{13}\text{C}_{\text{org}}$ values; Nold et al., 2013; Rico & Sheldon, 2019) become clearer with direct correlative analyses.

For LH sediments, MIS sediments, and MIS mat, S is significantly correlated with C_{org} ($p < .01$; Figure S3; Table 4), indicating that S in these environments is directly tied to organic matter, and making it difficult to disentangle the two cycles. Therefore, generally speaking, correlations between trace metals and S are inferred to reflect metal-organic matter cycling. In fact, among all correlative analyses between trace metals and C_{org} or S (Figures 3, 4, S4, and S5), there are only three metals for which there are significant

TABLE 2 Average^a trace metal contents for MIS sediments ($n = 38$), MIS mat ($n = 18$), and LH ($n = 22$) sediments

	MIS sediments	MIS mat	LH
Mn (ppm)	305 ± 47	225 ± 26	275 ± 83
Mn/Al (mmol/mol)	5.15 ± 0.68	4.33 ± 0.48	4.40 ± 1.42
U (ppm)	1.57 ± 0.12	1.47 ± 0.13	1.05 ± 0.18
U/Al (μmol/mol)	6.13 ± 0.49	6.55 ± 0.56	3.85 ± 0.70
V (ppm)	32.5 ± 2.9	28.4 ± 2.3	24.9 ± 2.9
V/Al (μmol/mol)	592 ± 14	592 ± 43	428 ± 52
Cd (ppm)	0.61 ± 0.11	0.46	0.39 ± 0.11
Cd/Al (μmol/mol)	4.99 ± 0.73	4.36 ± 0.79	3.03 ± 0.86
Zn (ppm)	55.7 ± 7.2	46.1 ± 6.7	35.1 ± 9.2
Zn/Al (mmol/mol)	0.79 ± 0.07	0.75 ± 0.12	0.47 ± 0.12
Ni (ppm)	21.3 ± 2.5	17.11 ± 2.4	13.0 ± 3.1
Ni/Al (mmol/mol)	0.34 ± 0.03	0.31 ± 0.04	0.19 ± 0.05
Cu (ppm)	20.8 ± 2.2	17.7 ± 3.1	9.17 ± 3.22
Cu/Al (mmol/mol)	0.30 ± 0.02	0.30 ± 0.05	0.13 ± 0.04
Mo (ppm)	0.48 ± 0.06	0.50 ± 0.08	0.25 ± 0.05
Mo/Al (μmol/mol)	4.73 ± 0.74	5.57 ± 0.93	2.27 ± 0.54 ^b

Abbreviations: LH, Lake Huron; MIS, Middle Island Sinkhole.

^aUncertainties are 1σ about the mean.

^bOne outlier removed for this average.

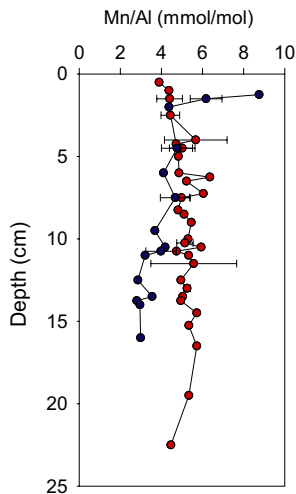
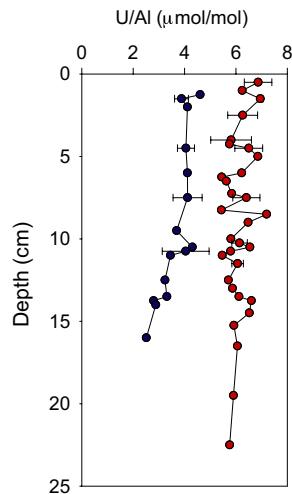
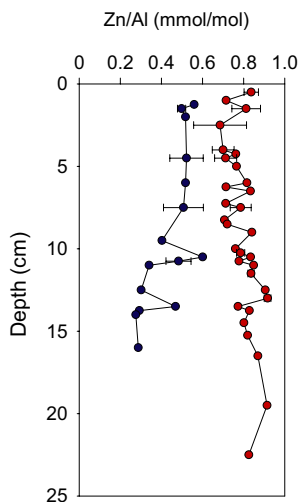
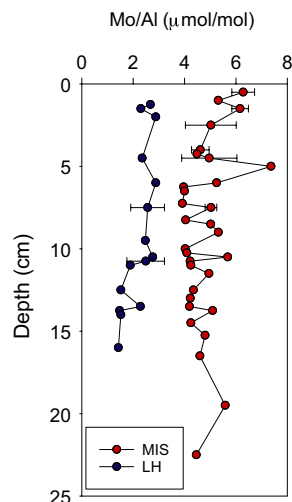
Ex. Oxide-forming trace metalEx. Paleoproxy for sub-oxic to anoxic conditionsEx. Micronutrient trace metalEx. Paleoproxy for euxinic conditions

FIGURE 1 Al-normalized depth profiles of the four different forms of trace metals explored in this study—oxide-forming trace metals (e.g., Mn), metals that accumulate under suboxic to anoxic conditions (e.g., U), micronutrient trace metals (e.g., Zn), and sulfide-complexed trace metals (e.g., Mo)—for Middle Island Sinkhole (MIS) and Lake Huron (LH). Values for a given depth are reported as means, with error bars representing variability (1σ) between different cores at particular depths ($n = 9$ for MIS, and $n = 8$ for LH)

correlations with C_{org} , but not with S: Mn, V, and Mo (discussed in detail in Sections 3.2.1, 3.2.2, and 3.2.4, respectively; Tables 3 and 4). Strong correlations between trace metals and organic C in LH ($p < .0005$; Table 3; Figures 3 and S4) indicate that metal burial is tied to organic matter burial in this oxic environment. Given that redox chemistry drives enhanced macronutrient burial in MIS sediments relative to LH sediments (Rico & Sheldon, 2019) and that the bulk of the trace metals are correlated with organic C in MIS mat and sediments (Table 3; Figures 3 and S4), redox is also a key control on enhanced trace metal burial for MIS. For most trace metals, there

are differences in slopes between the LH sediments, and the MIS mat and sediments (Table 3; Figures 3 and S4). Although both slopes are positive, the different slopes provide quantitative evidence of different metal- C_{org} relationships for the various abiotic-biotic redox regimes. Whether or not this is attributable to different redox chemistries (e.g., Rico & Sheldon, 2019), or a threshold value of organic C (~4%; Figures 3 and S4) is unclear. The presence of a break in slope indicates that in MIS, relative to LH, fewer metals are buried for the same amount of organic matter, potentially due to the abundance of organic matter (Nold et al., 2013; Rico & Sheldon, 2019), and/or a limited metal reservoir in MIS. However, without a quantification of trace metals in the Lake Huron water column vs. the groundwater that seeps into MIS, the mechanism for this break in slope remains unresolved. Similarly, although trace metal contents are greater in MIS than LH (Figures 1 and S1; Table 2), the contribution of trace metals from the groundwater to the trace metals in MIS mat and sediments is not constrained. Instead, by dividing select trace metals into four categories based upon their respective uses as redox and productivity proxies, we are able to differentiate the abiotic and biotic mechanisms for their burial in these freshwater environments.

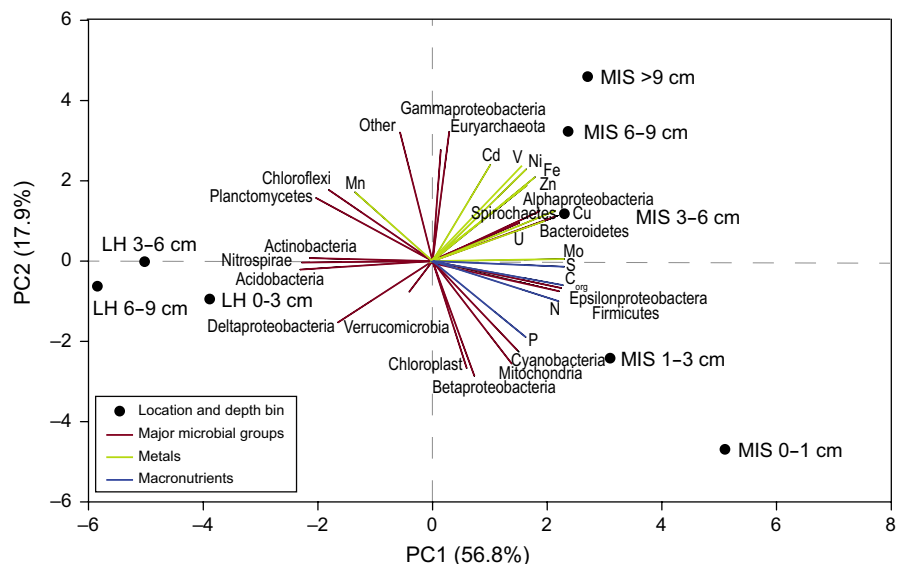
3.2 | Trace metals as redox and productivity proxies

3.2.1 | Manganese: an oxide-complexing trace metal

Oxidized Mn is predominantly found as a solid in the form of Mn-oxyhydroxides (MnO_2 and $MnOOH$; Calvert & Pedersen, 1993; Tribouillard et al., 2006). These Mn-oxyhydroxides can trap organic matter and trace metals (Tessier et al., 1996), which provides a mechanism for the correlations for each trace metal and Mn ($p < .05$), and between Mn and C_{org} ($r = .76$; $p < .0001$) in the oxic LH (Tables 3 and Figure S1; Figures 3 and S4). However, it is difficult to discern whether trace metals are adsorbed directly to the Mn-oxyhydroxide surfaces, or whether they require the additional presence of organic matter on Mn-oxyhydroxides surfaces for adsorption (e.g., Tessier et al., 1996). That being said, Mn is not correlated to S in LH sediments, MIS sediments, or MIS mat (Table 4; Figure 4); Mn-oxyhydroxide formation and deposition may be independent of S cycling, regardless of redox regime.

In reducing environments, Mn-oxyhydroxides can be dissolved, with Mn released into the water column as Mn(II) (Huerta-Diaz & Morse, 1992; Tribouillard et al., 2006). Dissolution of Mn in MIS mat and sediments may therefore limit the metal reservoir in MIS, resulting in the similarity between LH, MIS mat, and MIS sediment Mn contents (Table 2), and the lack of correlations between Mn and C_{org} as seen in Figure 3. Additionally, Mn-oxyhydroxides can also be transported through reducing waters to the sediment-water interface via a “particulate shuttle” (Algeo & Tribouillard, 2009). Such a mechanism in MIS and LH is corroborated by Mo vs. U covariation in these sediments (Rico et al., 2019). However, few

FIGURE 2 Principal component analysis demonstrating associations between trace metals and macronutrients, and relative abundances of major microbial groups for Middle Island Sinkhole (MIS; $n = 56$) and Lake Huron (LH; $n = 22$) sediments. LH and MIS sediments grouped by depth bins, and individual variable vectors are extended 10x for visualization. Macronutrient and Fe data from Rico and Sheldon (2019). Mo and U data from Rico et al. (2019). Relative abundances are from Kinsman-Costello et al. (2017)



correlations between metals and Mn in MIS sediments, and no correlations between metals and Mn in the MIS mat, indicate that Mn-oxyhydroxide deposition is not a key trace metal transport in these systems (Table S1). A rapid transport of Mn-oxyhydroxides from the oxygenated Lake Huron, through the low-oxygen MIS waters, and to MIS sediments would explain why Mn contents in MIS mat and sediments are similar to that of LH sediments (Table 2; Figure 1), and are not correlated to MIS C_{org} contents (Table 3; Figure 3). Thus, the burial of Mn in LH, MIS sediments, and MIS mat is in accordance with the current understanding of Mn-oxyhydroxide formation in oxic waters and rapid transport to the sediments.

The formation of Mn-oxyhydroxides in the LH sediments (and dissolution of these oxides in the MIS environments) provides an abiotic mechanism for why Mn is most associated to LH sediments of all of the trace metals in the PCA (Figure 2). There may also be a biological mechanism for this: Mn is required by oxygenic photosynthesis in the oxygen-evolving complex of photosystem II (Ferreira et al., 2004), and some of the microbial groups in high (>5%) abundance in LH sediments (e.g., Actinobacteria and Acidobacteria; Kinsman-Costello et al., 2017) have the capability to conduct aerobic respiration. Regardless, this work demonstrates that Mn serves as an oxygen indicator in freshwater, and possibly marine, environments.

3.2.2 | Proxies for suboxic–anoxic conditions

In the open ocean and in oxic sediments, U and V are present mainly as dissolved U(VI) and V(V), respectively, and are presumed to be dissociated from organic matter (e.g., Klinkhammer & Palmer, 1991; Tribovillard et al., 2006). Strong correlations in LH sediments between both V and Mn ($r = .91, p < .0001$), and a significant correlation between V and C_{org} ($r = .5, p < .05$), could be explained by the adsorption of V to Fe- and Mn-oxyhydroxides (Tables 4 and Figure S1; Figure 3; Calvert & Piper, 1984; Tribovillard et al., 2006). With Mn

cycling independent of S cycling (e.g., a lack of a correlation between Mn and S in LH sediments; Table S1), a Mn-oxyhydroxide shuttle of V to LH sediments is consistent with the lack of a correlation between V and S (Table 4; Figure S5). However, because U is not impacted by Fe- and Mn-oxyhydroxides (Tribovillard et al., 2006), this transport mechanism cannot explain the correlation between U/Al and C_{org} ($r = .91, p > .0001$), nor the correlation between U and S ($r = .78, p < .0001$) in LH sediments (Tables 3 and 4; Figures 3 and 4). Instead, these data suggest that, in some oxic sediments, U can also be buried readily via the formation of organometallic ligands in humic and fulvic acids (Figures 3 and S4). Alternatively, these correlations could be evidence for some reducing conditions within sediments beneath the oxic water column, which is partially corroborated by a depletion in pore water NO_3^- and increases in pore water Na^+ , Ca^{2+} , Mg^{2+} , SO_4^{2-} , and Cl^- with depth (>2 cm) in LH (Kinsman-Costello et al., 2017).

In suboxic to anoxic environments, U and V are both reduced and removed to sediments via the formation of organometallic ligands (Tribovillard et al., 2006). For U, this process can be promoted by the presence of bacterial sulfate reduction and subsequent free sulfide availability (sulfide production via bacterial sulfate reduction aids in the reduction of U to produce uraninite, the precursor to organometallic ligand formation; Klinkhammer & Palmer, 1991; McManus, Berelson, Klinkhammer, Hammond, & Holm, 2005). In comparison, the availability of free sulfides reduces V further, removing it from organometallic ligands (Morford & Emerson, 1999). A significant correlation between U and V and C_{org} ($r = .75, p < .0005, r = .9, p < .0001$, respectively; Tables 3 and 4; Figures 3 and S4), and no correlation between U or V and Mn (Table S1) where the bulk of the MIS bacterial sulfate reduction is taking place (the anoxic microbial mat; Kinsman-Costello et al., 2017; Voorhies et al., 2012), indicates no Mn-oxyhydroxide shuttle of these metals, but instead low enough oxygen to allow for U and V to complex with organic ligands, and limited sulfide production to disrupt the organometallic complexation of V.

In comparison, a correlation between Mn and V in MIS sediments ($r = .63, p < .0001$) demonstrates that Mn-oxyhydroxide transport

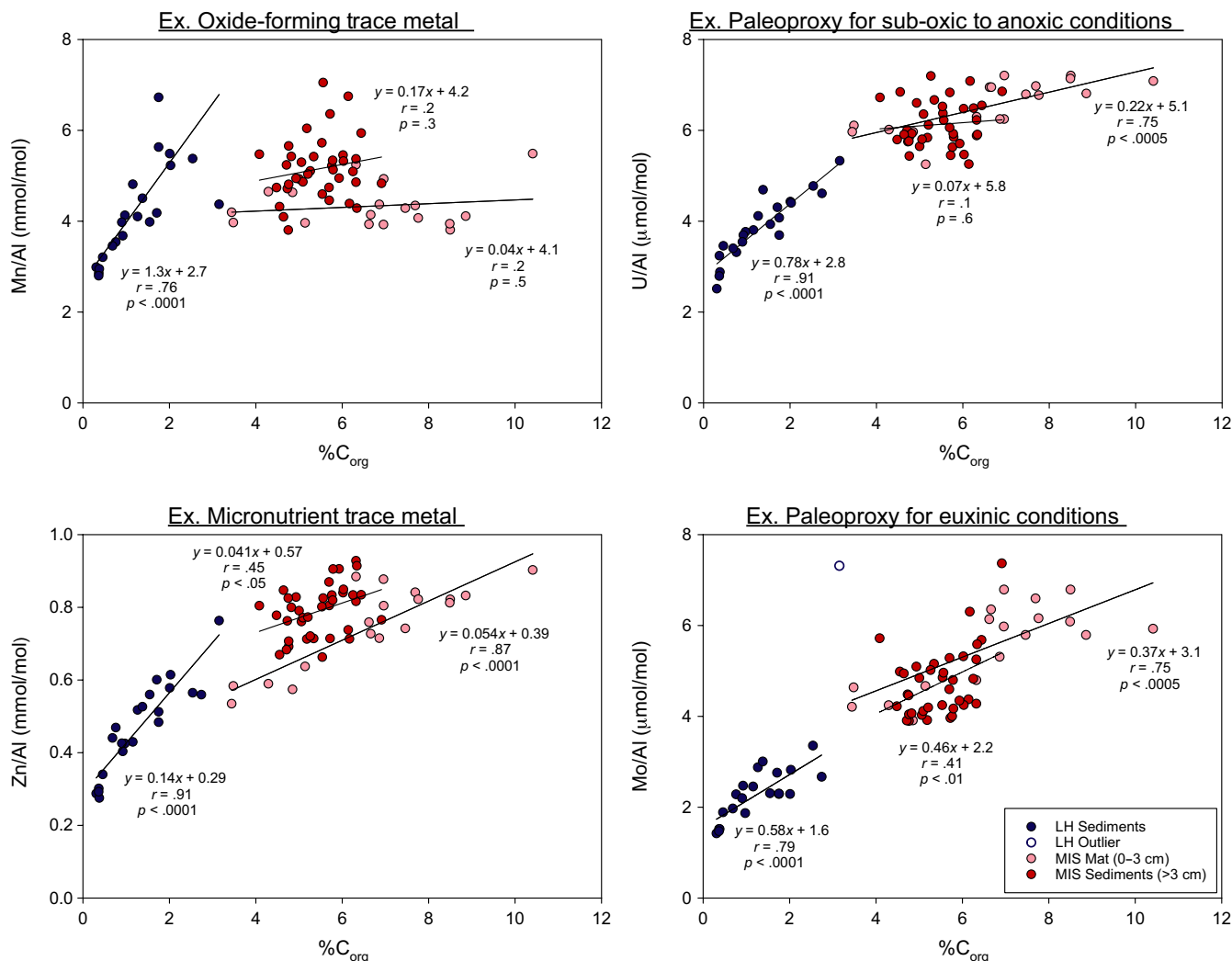


FIGURE 3 Correlations between Al-normalized trace metals and C_{org} for the four different forms of trace metals explored in this study—oxide-forming trace metals (e.g., Mn), metals that accumulate under suboxic to anoxic conditions (e.g., U), micronutrient trace metals (e.g., Zn), and sulfide-complexed trace metals (e.g., Mo)—in Lake Huron (LH) sediments, Middle Island Sinkhole (MIS) sediments, and MIS mat. Mo/Al LH outlier is not included in presented statistics. C_{org} data from Rico and Sheldon (2019). Mo and U data from Rico et al. (2019)

of V to sediment–water interface is playing a critical role in V cycling (Table S1). With no significant correlation between U and C_{org} in MIS sediments ($r = .1$, $p = .6$), it appears that U may be precipitating in MIS sediments as authigenic phases, separate from organic complexation (Algeo & Maynard, 2004; Tribovillard et al., 2006). Ultimately, the key differences in U and V cycling—response to sulfide (e.g., McManus et al., 2005), and the propensity to adsorb to Fe- and Mn-oxyhydroxides (e.g., Tribovillard et al., 2006)—lead to different burial pathways for these metals in LH sediments, MIS mat, and MIS sediments, with evidence Mn-oxyhydroxide shuttling dominating deposition of V, and organic complexation driving U burial.

3.2.3 | Micronutrient trace metals

In oxic environments, Cd, Zn, Ni, and Cu can act as micronutrients and are thus incorporated into organic matter or complex with humic/

fulvic acids (Calvert & Pedersen, 1993; Tribovillard et al., 2006); these metals can also adsorb to Fe- and Mn-oxyhydroxides and be transported to the sediments (Tessier et al., 1996). These metals act as expected in the oxic LH sediments, with contents strongly correlating to organic C ($p < .0001$; Table 3; Figures 3 and S4). In reducing sediments, they are mobilized and released into the water column during organic matter degradation and can complex with sulfide during bacterial sulfate reduction (Calvert & Pedersen, 1993; Huerta-Diaz & Morse, 1992). Although MIS mats are reducing, and therefore Cd, Zn, Ni, and Cu would be expected to be released into the water column (i.e., not associated with organic matter), there are still significant correlations between these metals and C_{org} ($p < .0001$; Table 3). This indicates that these metals are serving as micronutrients to the microbial mat itself and/or otherwise incorporated into the organic matter of the microbial mat. Significant relationships were also found in MIS sediments ($p < .05$; Table 3; Figures 3 and Figure S4), where sulfide availability would be expected to facilitate

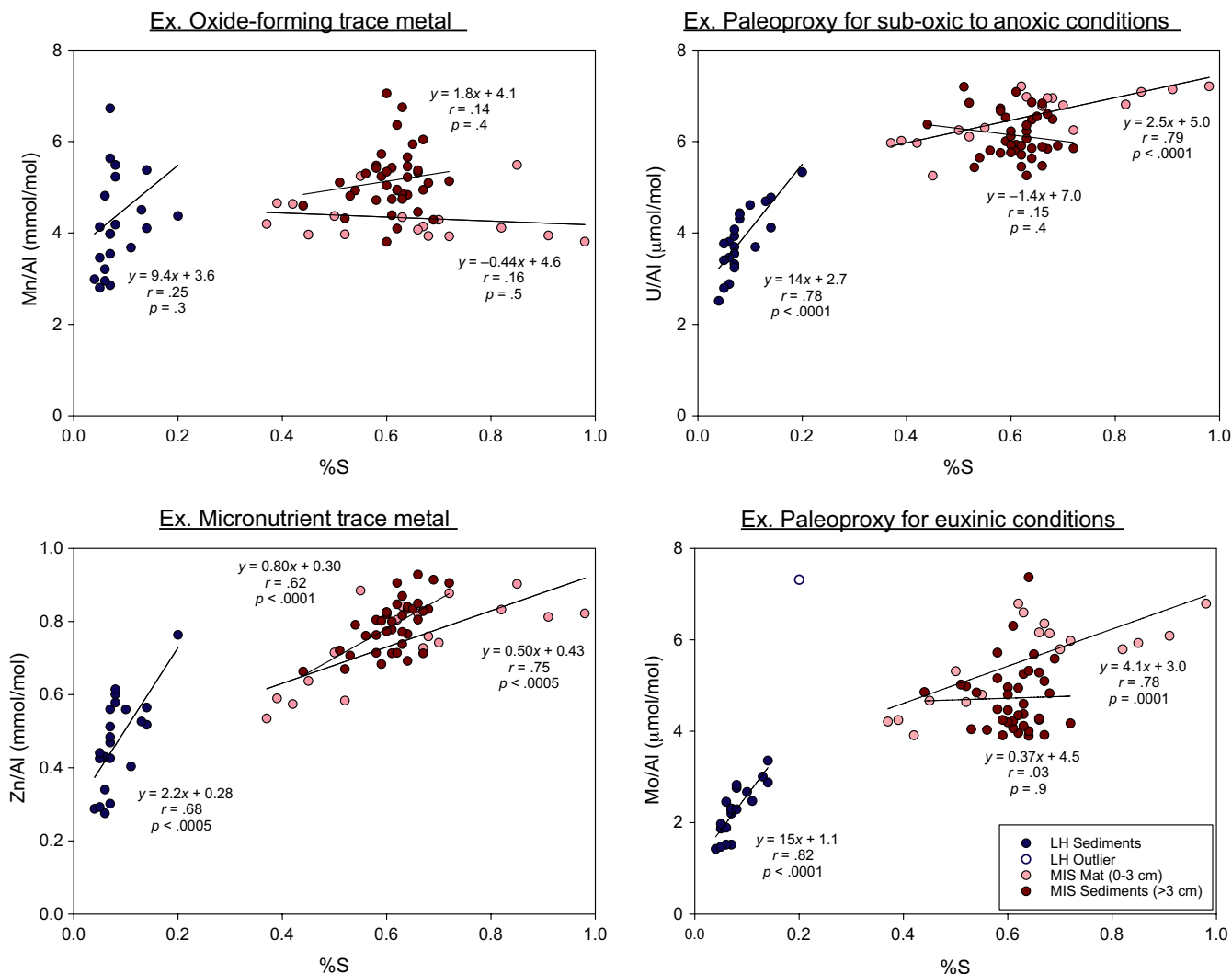


FIGURE 4 Correlations between Al-normalized trace metals and S for the four different forms of trace metals explored in this study—oxide-forming trace metals (e.g., Mn), metals that accumulate under suboxic to anoxic conditions (e.g., U), micronutrient trace metals (e.g., Zn), and sulfide-complexed trace metals (e.g., Mo)—in Lake Huron (LH) sediments, Middle Island Sinkhole (MIS) sediments, and MIS mat. Mo/Al LH outlier is not included in presented statistics. S data from Rico and Sheldon (2019). Mo and U data from Rico et al. (2019)

the formation of metal-sulfide complexes above metal-organics complexes. Alternatively, with enhanced organic C burial relative to LH and other Great Lakes sediments (Kinsman-Costello et al., 2017; Nold et al., 2013; Rico & Sheldon, 2019), MIS sediments may be sequestering and preserving organic matter efficiently enough that Cd, Zn, Ni, and Cu remain in metal-organic complexes. This also could be facilitated by the complexation of these metals with organic matter that is adsorbed to Mn-oxyhydroxides (e.g., Tessier et al., 1996), and rapid transport to the sediment-water interface; correlations between Mn, and Ni and Cu ($p < .001$) suggest shuttle by Mn-oxyhydroxides may play a role for micronutrient trace metal burial in MIS sediments (Table S1).

Cd, Zn, Ni, and Cu all plot in similar PC1 and PC2 space (Figure 2), which is expected because all of those elements are biotic micronutrients (Lepp, 1992; Moore et al., 2017; Tribovillard et al., 2006). These metals have varying affinities for organic ligands, sulfide,

and sorption to Fe- and Mn-oxyhydroxides (Huerta-Diaz, Tessier, & Carignan, 1998; Tessier et al., 1996; Tribovillard et al., 2006), which could explain both the variability in significance in correlations between the metals and C_{org} , S, and Mn (Tables 3, 4, and S1; Figures 3, 4, S4, S5) and their associations with one another in PCA space (Figure 2). However, the incorporation of these metals as enzymatic cofactors may also play a role, as they are highly variable across taxa and metabolisms (e.g., Moore et al., 2017). For example, bacterial cells have specific mechanisms for taking up Cu, Ni, and Zn (Lepp, 1992). In contrast, Cd is a nonessential element for most bacteria with no specific uptake mechanism (Silver, 1998), providing a biological mechanism for Cd to be least associated with (i.e., the farthest from) the microbial mat in the PCA (Figure 2). Conversely, the metal most closely associated with the microbial mat is Cu (Figure 2). Cu is critical in enzymes that catalyze microbial metabolisms such as nitrification, denitrification, aerobic oxidation

TABLE 3 Pearson's correlation coefficient (*r*) and significance (*p*-value) for Al-normalized trace metal contents vs. organic C contents for MIS sediments (*n* = 38), MIS mat (*n* = 18), and LH (*n* = 22) sediments. Relationships with significance < 0.05 are in bold

	MIS sediments		MIS mat		LH	
	<i>r</i>	<i>p</i>	<i>r</i>	<i>p</i>	<i>r</i>	<i>p</i>
Mn/Al	.2	.3	.2	.5	.76	<.0001
U/Al	.1	.6	.75	<.0005	.91	<.0001
V/Al	.4	<.05	.9	<.0001	.5	<.05
Cd/Al	.36	<.05	.88	<.0001	.90	<.0001
Zn/Al	.45	<.05	.87	<.0001	.91	<.0001
Ni/Al	.45	<.005	.95	<.001	.93	<.0001
Cu/Al	.50	<.005	.95	<.0001	.94	<.0001
Mo/Al	.41	<.01	.75	<.0005	.79 ^a	<.0001 ^a

Abbreviations: LH, Lake Huron; MIS, Middle Island Sinkhole.

^aOne outlier removed for these statistics.

TABLE 4 Pearson's correlation coefficient (*r*) and significance (*p*-value) for Al-normalized trace metal contents vs. S contents for MIS sediments (*n* = 38), MIS mat (*n* = 18), and LH (*n* = 22) sediments. Relationships with significance < 0.05 are in bold

	MIS sediments		MIS mat		LH	
	<i>r</i>	<i>p</i>	<i>r</i>	<i>p</i>	<i>r</i>	<i>p</i>
Mn/Al	.1	.4	.2	.5	.3	.3
U/Al	.2	.4	.79	<.001	.78	<.0001
V/Al	.59	<.0005	.89	<.0001	.07	.8
Cd/Al	.62	<.0001	.73	<.005	.69	<.0005
Zn/Al	.62	<.0001	.75	<.0005	.68	<.0005
Ni/Al	.68	<.0001	.75	<.0005	.71	<.0005
Cu/Al	.8	<.0001	.7	<.0001	.71	<.0005
Mo/Al	.03	.9	.78	<.0001	.82 ^a	<.0001 ^a

^aOne outlier removed for these statistics.

of ammonia, and aerobic respiration (Jelen et al., 2016). Given the breadth of metabolisms present in the MIS microbial mat (e.g., anoxygenic photosynthesis, oxygenic photosynthesis, and chemosynthesis; Voorhies et al., 2012; Kinsman-Costello et al., 2017), the association of Cu in the PCA with respect to the other micronutrient trace metals (Figure 2) may be indicative of its use by various metabolisms in the microbial mat.

3.2.4 | Molybdenum: a proxy for euxinia

In oxic waters, Mo is present as the unreactive molybdate anion (MoO_4^{2-}) and can be adsorbed to Fe- and Mn-oxyhydroxides (Calvert & Pedersen, 1993; Chappaz, Gobeil, & Tessier, 2008), which can explain the correlation between Mo and organic C ($r = .76$, $p < .0001$; Table 3; Figure 3) and the correlation between Mo and Mn ($r = .51$,

$p < .05$; Table S1) in LH sediments. Mo can also be transported to the sediments via Fe- and Mn-oxyhydroxides in reducing sediments (Algeo & Tribovillard, 2009; Scholz, Siebert, Dale, & Frank, 2017), and via complexation with organic matter (not associated with sulfide) in weakly sulfidic sediments (Tessin et al., 2018; Wagner, Chappaz, & Lyons, 2017). For the MIS mat, wherein sulfide is being produced via bacterial sulfate reduction but does not persist in high concentrations (Kinsman-Costello et al., 2017), there is a strong correlation between Mo and C_{org} ($r = .75$, $p < .0005$; Table 3; Figure 3), and no correlation between Mo and Mn (Table S1). These data indicate organic matter complexation driving Mo burial in MIS mat, not transport via Fe- and Mn-oxyhydroxides.

With free sulfides present, Mo can be converted into particle-reactive thiomolybdates ($\text{MoO}_x\text{S}_{(4-x)}^{2-}$) and scavenged with organic matter (Erickson & Helz, 2000; Tribovillard et al., 2006; Vorlicek, Chappaz, Groskreutz, Young, & Lyons, 2015), buried with Fe(II)-S phases (Helz, Erickson, & Vorlicek, 2014), and/or buried with organic matter independent of Fe or S (Dahl et al., 2017). As a result, a strong covariation between Mo and C_{org} has been demonstrated in euxinic basins and euxinic black shales (where "euxinia" is defined by persistent hydrogen sulfide in the water column; Algeo & Lyons, 2006; Helz & Vorlicek, 2019; Lyons, Anbar, Severmann, Scott, & Gill, 2009). The absolute concentrations of Mo in MIS samples are <1 ppm, values too low to be considered to be even anoxic according to the threshold of 20 ppm designated by Scott and Lyons (2012), in spite of measured dissolved O_2 levels consistent with anoxia (Ruberg et al., 2008). However, Hardisty et al. (2018) has demonstrated sedimentary Mo does not always effectively capture sulfide concentrations in pore waters beneath oxic and low oxygen water columns. Instead, using independent measurements—pore water sulfide concentrations up to 7 mM (Kinsman-Costello et al., 2017) and the MIS waters that are ferruginous rather than euxinic with respect to Fe (Rico & Sheldon, 2019)—verifies that MIS is not euxinic. Therefore, covariation between Mo and C_{org} ($r = .41$; $p < .01$) must be explained by something other than thiomolybdate formation or complexation with sulfide minerals. Using Mo-U covariation, Rico et al. (2019) found that Mo burial in MIS may follow the "particulate shuttle" pathway—wherein authigenic Mo is adsorbed to Mn- and Fe-(oxy)hydroxides, transported through the water column, and buried in sediments—as opposed to a burial pathway associated with euxinia.

This "particulate shuttle" pathway would explain significant correlations between Mo and organic C for MIS sediments ($p < .01$; Figure 3). However, Mo is negatively correlated to Mn ($r = -.32$, $p < .05$), indicating that the Mo in MIS sediments is not associated with Mn-oxyhydroxides. Correlations between Mo and C_{org} in MIS sediments are weaker than that of LH sediments and MIS mat (Table 3; Figure 3), and while Mo is correlated to S for LH sediments and MIS mat (attributable to the bulk of S being integrated with organic matter; Figure S3), Mo and S are not correlated for MIS sediments (Table 4; Figure 4). These data suggest that Mo and S may be associated with different pools of organic matter in MIS sediments.

Correlations between Mo and C_{org} in LH sediments, MIS mat, and MIS sediments (Figure 3) suggest a mechanism for Mo burial that is dependent on organic matter burial, regardless of redox regime. With current understanding of Mo isotope systematics largely dependent on the thiomolybdate burial pathway of Mo in euxinic environments (e.g., Neubert, Nägler, & Böttcher, 2008; Helz, Bura-Nakić, Mikac, & Ciglencić, 2011; Nägler, Neubert, Böttcher, Dellwig, & Schnetger, 2011), the propensity for Mo to be buried with organic matter independent of thiomolybdate formation (this work; Dahl et al., 2017; Wagner et al., 2017; Tessin et al., 2018) necessitates a reinterpretation of Mo isotope ratios in sediments (King, Perakis, & Pett-Ridge, 2018; Tessin et al., 2018).

3.3 | Relating microbiology to trace metal burial

Comparing the major microbial groups with relative abundances >5% for MIS mat (0–1 cm; $n = 17$), MIS sediments (>1 cm; $n = 87$), and LH sediments ($n = 11$) demonstrates substantial taxonomic overlap at the phylum level (e.g., Bacteroidetes, Betaproteobacteria, Verrucomicrobia) between the three sample regimes, irrespective of redox chemistry (Figure 5; Kinsman-Costello et al., 2017; Moore et al., 2017). Together, organisms represented by these phyla are capable of an extensive list of microbial metabolisms (Moore et al., 2017). This overlap could just be attributed to similar microbial assemblages across freshwater environments, or could in part be attributed to groundwater influence—groundwater directly interacts with MIS mat and sediments from above the sediment–water interface, whereas there is some subsurface groundwater influence in

LH sediments (as indicated by pore water ion chemistry; Kinsman-Costello et al., 2017).

Despite substantial taxonomic overlap between LH, MIS mat, and MIS sediments (Figure 5), there are some key phyla that are prominent for each of the environments. For example, as evident in Figures 2 and 5, relative abundances of the major phyla Nitrospirae, Actinobacteria, and Acidobacteria are the most associated to LH sediments; these are in high (>5%) abundance only in LH sediments (Figure 5; Kinsman-Costello et al., 2017). Additionally, Deltaproteobacteria is abundant only in LH sediments (>20%). In comparison, the MIS microbial mats include cyanobacteria (>20% abundance; Figure 5; Kinsman-Costello et al., 2017), which is corroborated by the strong association between cyanobacteria and MIS sediments where the active or buried microbial mat is present (0–3 cm depth; Figure 2; Nold et al., 2013; Rico & Sheldon, 2019; Voorhies et al., 2012). Additionally, the only phylum of Archaea with substantial presence—Euryarchaeota—is at relatively high abundance (>5%) in the MIS sediments (Figure 5) and is particularly associated with deeper MIS sediments (Figure 2). Euryarchaeota notably includes methanogens, which explains the production of methane in MIS sediments (Biddanda et al., 2012; Kinsman-Costello et al., 2017).

While metagenomics and metatranscriptomics work by Medina (2016) and Grim (2019) demonstrate greater metabolic diversity—and diversity in the use of electron acceptors—in MIS than in LH, this diversity is not evident when assessing phylum-level community assemblages, making it difficult to correlate trace metal burial to specific metabolic processes (e.g., the spread in microbial groups

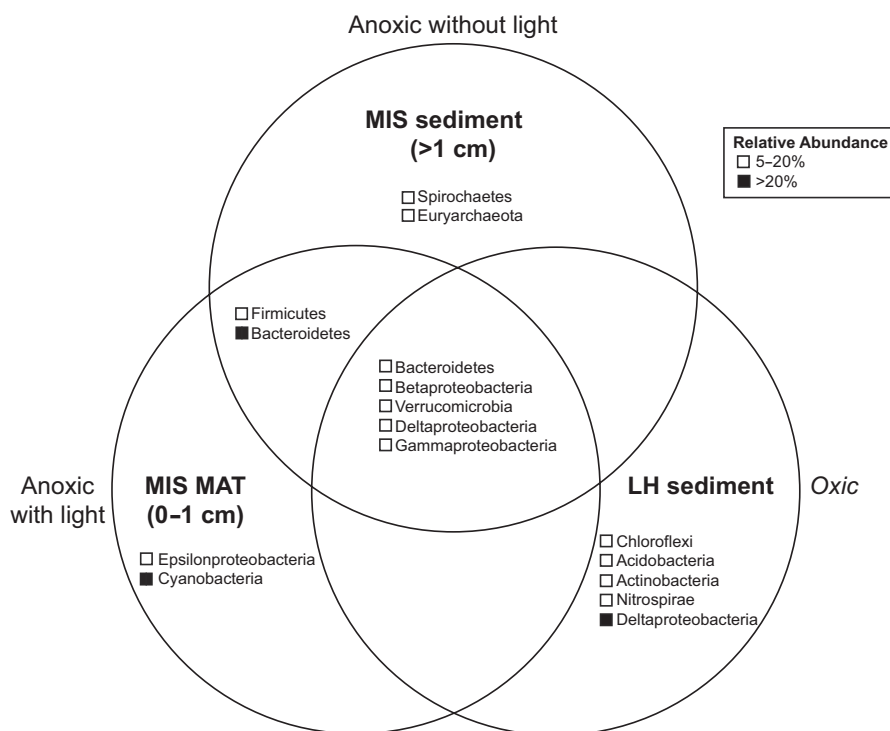


FIGURE 5 Venn diagram depicting the relative abundances of major microbial groups within the Middle Island Sinkhole (MIS) mat (0–1 cm; $n = 17$), MIS sediments (>1 cm; $n = 87$), and Lake Huron (LH) sediments ($n = 11$). Different symbols adjacent to the major microbial groups represent varying relative abundance in their respective locations. Relative abundances are from Kinsman-Costello et al. (2017)

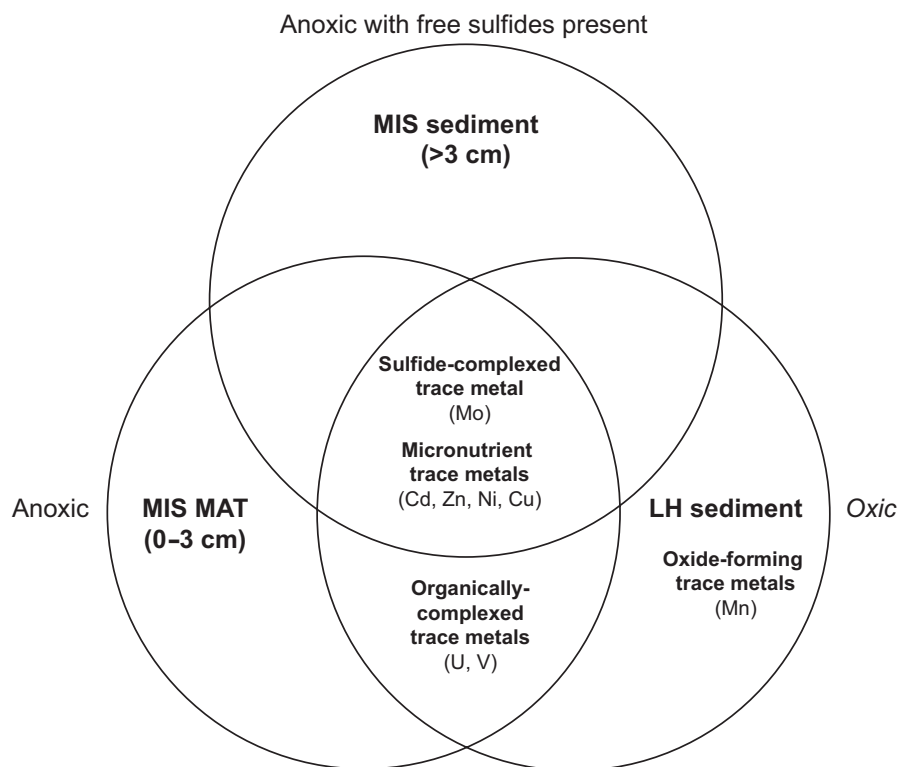


FIGURE 6 Venn diagram depicting the significant correlations ($p < .05$) between trace metals and C_{org} for the Middle Island Sinkhole (MIS) mat (0–3 cm; $n = 18$), MIS sediments (>3 cm; $n = 38$), and LH sediments ($n = 22$)

across Figure 2). At this biological scale, and considering total trace metal content (as opposed to speciation of metals), the direct relationships between microbial assemblages and metal burial in LH and MIS remain unresolved.

3.4 | Influence of MIS microbial mat on trace metal geochemistry

With similar microbial presence and water chemistry as has been inferred for the Proterozoic (Biddanda et al., 2012; Kinsman-Costello et al., 2017; Rico & Sheldon, 2019; Voorhies et al., 2012), the MIS is a useful modern analogue to consider the relationships between sediment trace metal geochemistry and microbial communities. Based on the presumed mechanisms behind trace metal burial in aquatic environments, and subsequently the ways in which trace metal geochemistry in ancient environments are used as paleoredox and paleoproductivity proxies, it was expected that the three abiotic/biotic regimes—oxic LH sediments, anoxic MIS mat, and anoxic MIS sediments with free sulfides present—would yield different relationships between trace metals and organic matter. However, for trace metals, there was significant overlap in their relationship with organic matter between the three regimes (Figures 3 and 6). Notably, there are no trace metal categories that feature significant correlations to C_{org} for only the MIS mat nor for the MIS sediments. Despite the differences in oxygen availability, sulfide availability, and microbial mat presence, there is no evidence that the presence of the MIS microbial mat generates vastly different impacts on the trace metal geochemistry in MIS. Instead, considering the ways in which

sediment metal geochemistry records biological processes may necessitate examining how biology influences tools such as metal speciation and metal isotope systematics.

4 | CONCLUSIONS

Trace metal data from MIS and LH reveal that the relationships between trace metals and organic matter are not consistent with what is expected from their use as paleoredox and paleoproductivity proxies. Of the types of trace metals assessed, evidence for Mn-oxyhydroxide formation and deposition in LH was the most consistent with expectations for burial mechanisms. In comparison, for U and V, which are generally anticipated to complex with organic matter under suboxic and anoxic conditions (Tribovillard et al., 2006), there was also evidence for organic matter complexation with U in oxic LH, and V burial dominated by Mn-oxyhydroxide shuttling in LH sediments and MIS sediments. Given that U accumulation is often used to reflect suboxic–anoxic (but not euxinic) environments in ancient environments (e.g., Algeo & Tribovillard, 2009), the accumulation of this metal in oxic environments has implications for how we interpret U geochemical data in the fossil record. Correlations between the micronutrient metals Cd, Zn, Ni, and Cu indicate complexation with organic matter regardless of redox, directly contradicting the hypothesized model of Algeo and Maynard (2004) and Tribovillard et al. (2006), which assumed no enrichment nor correlation under oxic–suboxic conditions. Importantly, this work demonstrates Mo covariation with organic C regardless of redox chemistry (Figure 3), which is decoupled from S cycling where free sulfides

are present (i.e., the MIS sediments). This is consistent with recent work highlighting organic matter as critical for Mo burial, independent of Fe or S (Dahl et al., 2017; Tessin et al., 2018), and informs our current understanding of Mo isotope systematics (e.g., Neubert et al., 2008; Helz et al., 2011; Nägler et al., 2011). Altogether, these results demonstrate a need for a greater understanding of the burial mechanisms for redox-sensitive trace metals under a variety of redox regimes that include suboxic and anoxic settings as well as euxinic ones, with special consideration for environments with significant microbiological presence.

ACKNOWLEDGMENTS

The authors wish to thank the NOAA Thunder Bay National Marine Sanctuary dive unit for their aide and expertise in accessing the field site and obtaining the cores. Thank you to Rebecca Dzombak and Clarissa Crist for their help in sample processing. This research was funded by the NSF GRFP to KIR, a University of Michigan Department of EES Turner Award to KIR, and a Sokol Foundation grant to NDS. We thank Noah Planavsky and the two anonymous reviewers for their helpful comments and suggestions.

ORCID

Kathryn I. Rico  <https://orcid.org/0000-0003-2761-8663>

Nathan D. Sheldon  <https://orcid.org/0000-0003-3371-0036>

REFERENCES

- Algeo, T. J., & Lyons, T. W. (2006). Mo-total organic carbon covariation in modern anoxic marine environments: Implications for analysis of paleoredox and paleohydrographic conditions. *Paleoceanography*, 21(1), 23 pp. <https://doi.org/10.1029/2004PA001112>
- Algeo, T. J., & Maynard, J. B. (2004). Trace-element behavior and redox facies in core shales of Upper Pennsylvanian Kansas-type cyclothems. *Chemical Geology*, 206(3–4), 289–318. <https://doi.org/10.1016/j.chemgeo.2003.12.009>
- Algeo, T. J., & Tribovillard, N. (2009). Environmental analysis of paleoceanographic systems based on molybdenum-uranium covariation. *Chemical Geology*, 268(3–4), 211–225. <https://doi.org/10.1016/j.chemgeo.2009.09.001>
- Biddanda, B. A., Nold, S. C., Dick, G. J., Kendall, S. T., Vail, J. H., Ruberg, S. A., & Green, C. M. (2012). Rock, water, microbes: Underwater sinkholes in Lake Huron are habitats for ancient microbial life. *Nature Education Knowledge*, 3(10), 13. <https://www.nature.com/scitable/knowledge/library/rock-water-microbes-underwater-sinkholes-in-lake-25851285/>
- Brocks, J. J., Jarrett, A. J. M., Sirantoine, E., Hallmann, C., Hoshino, Y., & Liyanage, T. (2017). The rise of algae in Cryogenian oceans and the emergence of animals. *Nature*, 548(7669), 578–581. <https://doi.org/10.1038/nature23457>
- Calvert, S. E., & Pedersen, T. F. (1993). Geochemistry of recent oxic and anoxic marine sediments: Implications for the geological record. *Marine Geology*, 113(1–2), 67–88. [https://doi.org/10.1016/0025-3227\(93\)90150-T](https://doi.org/10.1016/0025-3227(93)90150-T)
- Calvert, S. E., & Piper, D. Z. (1984). Geochemistry of ferromanganese nodules from DOMES site a, Northern Equatorial Pacific: Multiple diagenetic metal sources in the deep sea. *Geochimica et Cosmochimica Acta*, 48(10), 1913–1928. [https://doi.org/10.1016/0016-7037\(84\)90374-0](https://doi.org/10.1016/0016-7037(84)90374-0)
- Chappaz, A., Gobeil, C., & Tessier, A. (2008). Geochemical and anthropogenic enrichments of Mo in sediments from perennially oxic and seasonally anoxic lakes in Eastern Canada. *Geochimica et Cosmochimica Acta*, 72(1), 170–184. <https://doi.org/10.1016/j.gca.2007.10.014>
- Dahl, T. W., Chappaz, A., Hoek, J., McKenzie, C. J., Svane, S., & Canfield, D. E. (2017). Evidence of molybdenum association with particulate organic matter under sulfidic conditions. *Geobiology*, 15(2), 311–323. <https://doi.org/10.1111/gbi.12220>
- Erickson, B. E., & Helz, G. R. (2000). Molybdenum(VI) speciation in sulfidic waters: Stability and lability of thiomolybdates. *Geochimica et Cosmochimica Acta*, 64(7), 1149–1158. [https://doi.org/10.1016/S0016-7037\(99\)00423-8](https://doi.org/10.1016/S0016-7037(99)00423-8)
- Farquhar, J., Bao, H., & Thiemens, M. (2000). Atmospheric influence of earth's earliest sulfur cycle. *Science*, 289, 756–758. <https://doi.org/10.1126/science.289.5480.756>
- Ferreira, K. N., Iverson, T. M., Maghlaoui, K., Barber, J., & Iwata, S. (2004). Architecture of the photosynthetic oxygen-evolving center. *Science*, 303, 1831–1839.
- Grim, S. (2019). *Genomic and functional investigations into seasonally-impacted and morphologically-distinct anoxygenic photosynthetic cyanobacterial mats*. Doctoral dissertation. University of Michigan.
- Hamilton, T. L., Welander, P. V., Albrecht, H. L., Fulton, J. M., Schaperdoth, I., Bird, L. R., ... Macalady, J. L. (2017). Microbial communities and organic biomarkers in a Proterozoic-analog sinkhole. *Geobiology*, 15(6), 784–797. <https://doi.org/10.1111/gbi.12252>
- Hammer, Ø., Harper, D. A. T., & Ryan, P. D. (2001). PAST: Paleontological statistics software package for education and data analysis. *Paleontologia Electronica*, 4(1), 1–9.
- Hardisty, D. S., Lyons, T. W., Riedinger, N., Isson, T. T., Owens, J. D., Aller, R. C., ... Johnston, D. T. (2018). An evaluation of sedimentary molybdenum and iron as proxies for pore fluid paleoredox conditions. *American Journal of Science*, 318(5), 527–556. <https://doi.org/10.2475/05.2018.04>
- Hasiotis, S. T., Brake, S. S., Dannelly, H. K., & Duncan, A. (2001). Eukaryote-dominated microbial communities that build iron-stromatolites in acid mine drainage, Western Indiana: An analog for proterozoic banded iron formations and oxygenation of the early atmosphere. Lunar and Planetary Science Conference, Houston, TX, USA, 32.
- Helz, G. R., Bura-Nakić, E., Mikac, N., & Ciglenciki, I. (2011). New model for molybdenum behavior in euxinic waters. *Chemical Geology*, 284(3–4), 323–332. <https://doi.org/10.1016/j.chemgeo.2011.03.012>
- Helz, G. R., Erickson, B. E., & Vorlicek, T. P. (2014). Stabilities of thiomolybdate complexes of iron; Implications for retention of essential trace elements (Fe, Cu, Mo) in sulfidic waters. *Metallomics*, 6(6), 1131–1140. <https://doi.org/10.1039/c3mt00217a>
- Helz, G. R., & Vorlicek, T. P. (2019). Precipitation of molybdenum from euxinic waters and the role of organic matter. *Chemical Geology*, 509(January), 178–193. <https://doi.org/10.1016/j.chemgeo.2019.02.001>
- Huerta-Diaz, M. A., & Morse, J. W. (1992). Pyritization of trace metals in anoxic marine sediments. *Geochimica et Cosmochimica Acta*, 56(7), 2681–2702. [https://doi.org/10.1016/0016-7037\(92\)90353-K](https://doi.org/10.1016/0016-7037(92)90353-K)
- Huerta-Diaz, M. A., Tessier, A., & Carignan, R. (1998). Geochemistry of trace metals associated with reduced sulfur in freshwater sediments. *Applied Geochemistry*, 13(2), 213–233. [https://doi.org/10.1016/S0883-2927\(97\)00060-7](https://doi.org/10.1016/S0883-2927(97)00060-7)
- Jelen, B. I., Giovannelli, D., & Falkowski, P. G. (2016). The role of microbial electron transfer in the coevolution of the biosphere and geosphere. *Annual Review of Microbiology*, 70(1), 45–62. <https://doi.org/10.1146/annurev-micro-102215-095521>
- King, E. K., Perakis, S. S., & Pett-Ridge, J. C. (2018). Molybdenum isotope fractionation during adsorption to organic matter. *Geochimica et Cosmochimica Acta*, 222, 584–598. <https://doi.org/10.1016/j.gca.2017.11.014>

- Kinsman-Costello, L. E., Sheik, C. S., Sheldon, N. D., Burton, G. A., Costello, D., Marcus, D. N., ... Dick, G. J. (2017). Groundwater shapes sediment biogeochemistry and microbial diversity in a submerged sinkhole. *Geobiology*, 15(2), 225–239. <https://doi.org/10.1038/natur-e04068>
- Klinkhammer, G. P., & Palmer, M. R. (1991). Uranium in the oceans: Where it goes and why. *Geochimica et Cosmochimica Acta*, 55(7), 1799–1806. [https://doi.org/10.1016/0016-7037\(91\)90024-Y](https://doi.org/10.1016/0016-7037(91)90024-Y)
- Knoll, A. H. (2015). Paleobiological perspectives on early microbial evolution. *Cold Spring Harbor Perspectives in Biology*, 7(7), 1–17. <https://doi.org/10.1101/cshperspect.a018093>
- Konhauer, K. O., Phoenix, V. R., Bottrell, S. H., Adams, D. G., & Head, I. M. (2001). Microbial-silica interactions in Icelandic hot spring sinter: Possible analogues for some Precambrian siliceous stromatolites. *Sedimentology*, 48(2), 415–433. <https://doi.org/10.1046/j.1365-3091.2001.00372.x>
- Lepp, N. W. (1992). Uptake and accumulation of metals in bacteria and fungi. In D. C. Adriano (Ed.), *Biogeochemistry of trace metals* (pp. 277–298). Boca Raton, FL: Lewis Publishers.
- Lyons, T. W., Anbar, A. D., Severmann, S., Scott, C., & Gill, B. C. (2009). Tracking euxinia in the ancient ocean: A multiproxy perspective and proterozoic case study. *Annual Review of Earth and Planetary Sciences*, 37(1), 507–534. <https://doi.org/10.1146/annurev.earth.36.031207.124233>
- Lyons, T. W., Reinhard, C. T., & Planavsky, N. J. (2014). The rise of oxygen in Earth's early ocean and atmosphere. *Nature*, 506(7488), 307–315. <https://doi.org/10.1038/nature13068>
- McManus, J., Berelson, W. M., Klinkhammer, G. P., Hammond, D. E., & Holm, C. (2005). Authigenic uranium: Relationship to oxygen penetration depth and organic carbon rain. *Geochimica et Cosmochimica Acta*, 69(1), 95–108. <https://doi.org/10.1016/j.gca.2004.06.023>
- Medina, M. (2016). *Genomic and transcriptomic evidence for niche partitioning among sulfate-reducing bacteria in redox-stratified cyanobacterial mats of the Middle Island Sinkhole*. Master's thesis, University of Michigan.
- Miller, A. J., Strauss, J. V., Halverson, G. P., Macdonald, F. A., Johnston, D. T., & Sperling, E. A. (2017). Tracking the onset of phanerozoic-style redox-sensitive trace metal enrichments: new results from basal Ediacaran post-glacial strata in NW Canada. *Chemical Geology*, 457, 24–37. <https://doi.org/10.1016/j.chemgeo.2017.03.010>
- Moore, E. K., Jelen, B. I., Giovannelli, D., Raanan, H., & Falkowski, P. G. (2017). Metal availability and the expanding network of microbial metabolisms in the Archaean eon. *Nature Geoscience*, 10(9), 629–636. <https://doi.org/10.1038/ngeo3006>
- Morford, J. L., & Emerson, S. (1999). The geochemistry of redox sensitive trace metals in sediments. *Geochimica et Cosmochimica Acta*, 63(11–12), 1735–1750. [https://doi.org/10.1016/S0016-7037\(99\)00126-X](https://doi.org/10.1016/S0016-7037(99)00126-X)
- Nägler, T. F., Neubert, N., Böttcher, M. E., Dellwig, O., & Schnetger, B. (2011). Molybdenum isotope fractionation in pelagic euxinia: Evidence from the modern Black and Baltic Seas. *Chemical Geology*, 289(1–2), 1–11. <https://doi.org/10.1016/j.chemgeo.2011.07.001>
- Neubert, N., Nägler, T. F., & Böttcher, M. E. (2008). Sulfidity controls molybdenum isotope fractions into euxinic sediments: Evidence from the modern Black Sea. *Geology*, 36(10), 775–778. <https://doi.org/10.1130/G24959A.1>
- Nguyen, K., Love, G. D., Zumberge, J. A., Kelly, A. E., Owens, J. D., Rohrsen, M. K., ... Lyons, T. W. (2019). Absence of biomarker evidence for early eukaryotic life from the Mesoproterozoic Roper Group: Searching across a marine redox gradient in mid-Proterozoic habitability. *Geobiology*, 17(3), 247–260. <https://doi.org/10.1111/gbi.12329>
- Noffke, N., & Awramik, S. M. (2013). Stromatolites and MISS-differences between relatives. *GSA Today*, 23(9), 4–9. <https://doi.org/10.1130/GSATG187A.1>
- Nold, S. C., Bellecourt, M. J., Kendall, S. T., Ruberg, S. A., Sanders, T. G., Klump, J. V., & Biddanda, B. A. (2013). Underwater sinkhole sediments sequester Lake Huron's carbon. *Biogeochemistry*, 115(1–3), 235–250. <https://doi.org/10.1007/s10533-013-9830-8>
- Oksanen, K., Blanchet, F. G., Kindt, R., Legendre, P., Minchin, P. R., Ohara, R. B., & Oksanen, M. J. (2013). Package 'vegan'. Community ecology package, version 2.5-5.
- Planavsky, N. J., Slack, J. F., Cannon, W. F., O'Connell, B., Isson, T. T., Asael, D., ... Bekker, A. (2018). Evidence for episodic oxygenation in a weakly redox-buffered deep mid-Proterozoic ocean. *Chemical Geology*, 483, 581–594. <https://doi.org/10.1016/j.chemgeo.2018.03.028>
- Raiswell, R., & Canfield, D. E. (2012). The iron biogeochemical cycle past and present. *Geochemical Perspectives*, 1(1), 1–220. <https://doi.org/10.7185/geochempersp.1.1>
- Raiswell, R., Hardisty, D. S., Lyons, T. W., Canfield, D. E., Owens, J. D., Planavsky, N. J., ... Reinhard, C. T. (2018). The iron paleoredox proxies: A guide to the pitfalls, problems and proper practice. *American Journal of Science*, 318(5), 491–526. <https://doi.org/10.2475/05.2018.03>
- Reinhard, C. T., Planavsky, N. J., Robbins, L. J., Partin, C. A., Gill, B. C., Lalonde, S. V., ... Lyons, T. W. (2013). Proterozoic ocean redox and biogeochemical stasis. *Proceedings of the National Academy of Sciences*, 110(14), 5357–5362. <https://doi.org/10.1073/pnas.1208622110>
- Rico, K. I., & Sheldon, N. D. (2019). Nutrient and iron cycling in a modern analogue for the redoxcline of a Proterozoic ocean shelf. *Chemical Geology*, 511, 42–50. <https://doi.org/10.1016/j.chemgeo.2019.02.032>
- Rico, K. I., Sheldon, N. D., Gallagher, T. M., & Chappaz, A. (2019). Redox chemistry and molybdenum burial in a Mesoproterozoic Lake. *Geophysical Research Letters*, 46, 5871–5878. <https://doi.org/10.1029/2019GL083316>
- Rothschild, L. J. (1991). A model for diurnal patterns of carbon fixation in a Precambrian microbial mat based on a modern analog. *BioSystems*, 25(1–2), 13–23. [https://doi.org/10.1016/0303-2647\(91\)90009-A](https://doi.org/10.1016/0303-2647(91)90009-A)
- Ruberg, S. A., Kendall, S. T., Biddanda, B. A., Black, T., Nold, S. C., Lusardi, W. R., ... Constant, S. A. (2008). Observations of the Middle Island Sinkhole and Glacial Creation of 400 million years. *Marine Technology Society Journal*, 42(4), 12–21.
- Scholz, F., Siebert, C., Dale, A. W., & Frank, M. (2017). Intense molybdenum accumulation in sediments underneath a nitrogenous water column and implications for the reconstruction of paleo-redox conditions based on molybdenum isotopes. *Geochimica et Cosmochimica Acta*, 213, 400–417. <https://doi.org/10.1016/j.gca.2017.06.048>
- Scott, C., & Lyons, T. W. (2012). Contrasting molybdenum cycling and isotopic properties in euxinic versus non-euxinic sediments and sedimentary rocks: Refining the paleoproxies. *Chemical Geology*, 324–325, 19–27. <https://doi.org/10.1016/j.chemgeo.2012.05.012>
- Silver, S. (1998). Genes for all metals—a bacterial view of the Periodic Table. *Journal of Industrial Microbiology and Biotechnology*, 20(1), 1–12. <https://doi.org/10.1038/sj.jim.2900483>
- Sperling, E. A., Halverson, G. P., Knoll, A. H., Macdonald, F. A., & Johnston, D. T. (2013). A basin redox transect at the dawn of animal life. *Earth and Planetary Science Letters*, 371–372, 143–155. <https://doi.org/10.1016/j.epsl.2013.04.003>
- Tessier, A., Fortin, D., Belzile, N., DeVitre, R. R., & Leppard, G. G. (1996). Metal sorption to diagenetic iron and manganese oxyhydroxides and associated organic matter: Narrowing the gap between field and laboratory measurements. *Geochimica et Cosmochimica Acta*, 60(3), 387–404. [https://doi.org/10.1016/0016-7037\(95\)00413-0](https://doi.org/10.1016/0016-7037(95)00413-0)
- Tessin, A., Chappaz, A., Hendy, I., & Sheldon, N. (2018). Molybdenum speciation as a paleo-redox proxy: A case study from Late Cretaceous Western Interior Seaway black shales. *Geology*, 47(1), 59–62. <https://doi.org/10.1130/g45785.1>
- Tribouillard, N., Algeo, T. J., Lyons, T., & Riboulleau, A. (2006). Trace metals as paleoredox and paleoproductivity proxies: An update.

- Chemical Geology*, 232(1–2), 12–32. <https://doi.org/10.1016/j.chemgeo.2006.02.012>
- Van der Weijden, C. H. (2002). Pitfalls of normalization of marine geochemical data using a common divisor. *Marine Geology*, 184, 167–187.
- Voorhies, A. A., Biddanda, B. A., Kendall, S. T., Jain, S., Marcus, D. N., Nold, S. C., ... Dick, G. J. (2012). Cyanobacterial life at low O₂: Community genomics and function reveal metabolic versatility and extremely low diversity in a Great Lakes sinkhole mat. *Geobiology*, 10(3), 250–267. <https://doi.org/10.1111/j.1472-4669.2012.00322.x>
- Vorlicek, T. P., Chappaz, A., Groskreutz, L. M., Young, N., & Lyons, T. W. (2015). A new analytical approach to determining Mo and Re speciation in sulfidic waters. *Chemical Geology*, 403, 52–57. <https://doi.org/10.1016/j.chemgeo.2015.03.003>
- Wagner, M., Chappaz, A., & Lyons, T. W. (2017). Molybdenum speciation and burial pathway in weakly sulfidic environments: Insights from XAFS. *Geochimica et Cosmochimica Acta*, 206, 18–29. <https://doi.org/10.1016/j.gca.2017.02.018>
- Zheng, Y., Anderson, R. F., Van Geen, A., & Kuwabara, J. (2000). Authigenic molybdenum formation in marine sediments: A link to pore water

sulfide in the Santa Barbara Basin. *Geochimica et Cosmochimica Acta*, 64(24), 4165–4178. [https://doi.org/10.1016/S0016-7037\(00\)00495-6](https://doi.org/10.1016/S0016-7037(00)00495-6)

SUPPORTING INFORMATION

Additional supporting information may be found online in the Supporting Information section.

How to cite this article: Rico KI, Sheldon ND, Kinsman-Costello LE. Associations between redox-sensitive trace metals and microbial communities in a Proterozoic ocean analogue. *Geobiology*. 2020;18:462–475. <https://doi.org/10.1111/gbi.12388>